



A Dynamical Model of a Crystal Structure

Lawrence Bragg; J. F. Nye

Proceedings of the Royal Society of London. Series A, Mathematical and Physical Sciences, Vol. 190, No. 1023. (Sep. 9, 1947), pp. 474-481.

Stable URL:

<http://links.jstor.org/sici?sici=0080-4630%2819470909%29190%3A1023%3C474%3AADMOAC%3E2.0.CO%3B2-D>

Proceedings of the Royal Society of London. Series A, Mathematical and Physical Sciences is currently published by The Royal Society.

Your use of the JSTOR archive indicates your acceptance of JSTOR's Terms and Conditions of Use, available at <http://www.jstor.org/about/terms.html>. JSTOR's Terms and Conditions of Use provides, in part, that unless you have obtained prior permission, you may not download an entire issue of a journal or multiple copies of articles, and you may use content in the JSTOR archive only for your personal, non-commercial use.

Please contact the publisher regarding any further use of this work. Publisher contact information may be obtained at <http://www.jstor.org/journals/rsl.html>.

Each copy of any part of a JSTOR transmission must contain the same copyright notice that appears on the screen or printed page of such transmission.

The JSTOR Archive is a trusted digital repository providing for long-term preservation and access to leading academic journals and scholarly literature from around the world. The Archive is supported by libraries, scholarly societies, publishers, and foundations. It is an initiative of JSTOR, a not-for-profit organization with a mission to help the scholarly community take advantage of advances in technology. For more information regarding JSTOR, please contact support@jstor.org.

REFERENCES

- Andrade, E. N. da C. 1934 *Phil. Mag.* ser. 7, **17**, 497, 698.
 Born, M. & Green, H. S. 1946 *Proc. Roy. Soc. A*, **188**, 10.
 Chapman, S. 1912 *Phil. Trans. A*, **211**, 433.
 Chapman, S. 1916 *Phil. Trans. A*, **216**, 279.
 Chapman, S. & Cowling, T. G. 1939 *The mathematical theory of non-uniform gases*. Camb. Univ. Press.
 Enskog, D. 1911 *Phys. Z.* **12**, 56, 533.
 Enskog, D. 1917 Uppsala Diss.
 Ewell, R. H. & Eyring, H. 1937 *J. Chem. Phys.* **5**, 726.
 Fürth, R. 1941 *Proc. Camb. Phil. Soc.* **37**, 281.
 Green, H. S. 1947 *Proc. Roy. Soc. A*, **189**, 103.
 de Guzman Carrancio J. 1913 *An. Soc. Esp. Fis. Quim.* **11**, 353.
 Hilbert, D. 1912 *Math. Ann.* **72**, 562.
 Kahn, B. 1938 Utrecht Diss.
 Lennard-Jones, J. E. 1924 *Proc. Roy. Soc. A*, **106**, 463.

A dynamical model of a crystal structure

BY SIR LAWRENCE BRAGG, F.R.S. AND J. F. NYE

Cavendish Laboratory, University of Cambridge

(Received 9 January 1947—Read 19 June 1947)

[Plates 8 to 21]

The crystal structure of a metal is represented by an assemblage of bubbles, a millimetre or less in diameter, floating on the surface of a soap solution. The bubbles are blown from a fine pipette beneath the surface with a constant air pressure, and are remarkably uniform in size. They are held together by surface tension, either in a single layer on the surface or in a three-dimensional mass. An assemblage may contain hundreds of thousands of bubbles and persists for an hour or more. The assemblages show structures which have been supposed to exist in metals, and simulate effects which have been observed, such as grain boundaries, dislocations and other types of fault, slip, recrystallization, annealing, and strains due to 'foreign' atoms.

1. THE BUBBLE MODEL

Models of crystal structure have been described from time to time in which the atoms are represented by small floating or suspended magnets, or by circular disks floating on a water surface and held together by the forces of capillary attraction. These models have certain disadvantages; for instance, in the case of floating objects in contact, frictional forces impede their free relative movement. A more serious disadvantage is that the number of components is limited, for a large number of components is required in order to approach the state of affairs in a real crystal.

The present paper describes the behaviour of a model in which the atoms are represented by small bubbles from 2·0 to 0·1 mm. in diameter floating on the surface of a soap solution. These small bubbles are sufficiently persistent for experiments lasting an hour or more, they slide past each other without friction, and they can be produced in large numbers. Some of the illustrations in this paper were taken from assemblages of bubbles numbering 100,000 or more. The model most nearly represents the behaviour of a metal structure, because the bubbles are of one type only and are held together by a general capillary attraction, which represents the binding force of the free electrons in the metal. A brief description of the model has been given in the *Journal of Scientific Instruments* (Bragg 1942*b*).

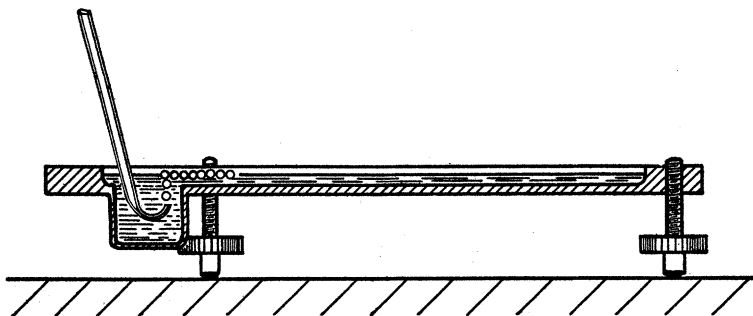


FIGURE 1. Apparatus for producing rafts of bubbles.

2. METHOD OF FORMATION

The bubbles are blown from a fine orifice, beneath the surface of a soap solution. We have had the best results with a solution the formula of which was given to us by Mr Green of the Royal Institution. 15·2 c.c. of oleic acid (pure redistilled) is well shaken in 50 c.c. of distilled water. This is mixed thoroughly with 73 c.c. of 10 % solution of tri-ethanolamine and the mixture made up to 200 c.c. To this is added 164 c.c. of pure glycerine. It is left to stand and the clear liquid is drawn off from below. In some experiments this was diluted in three times its volume of water to reduce viscosity. The orifice of the jet is about 5 mm. below the surface. A constant air pressure of 50 to 200 cm. of water is supplied by means of two Winchester flasks. Normally the bubbles are remarkably uniform in size. Occasionally they issue in an irregular manner, but this can be corrected by a change of jet or of pressure. Unwanted bubbles can easily be destroyed by playing a small flame over the surface. Figure 1 shows the apparatus. We have found it of advantage to blacken the bottom of the vessel, because details of structure, such as grain boundaries and dislocations, then show up more clearly.

Figure 2, plate 8, shows a portion of a 'raft' or two-dimensional crystal of bubbles. Its regularity can be judged by looking at the figure in a glancing direction. The size of the bubbles varies with the aperture, but does not appear to vary to any marked degree with the pressure or the depth of the orifice beneath the surface.

The main effect of increasing the pressure is to increase the rate of issue of the bubbles. As an example, a thick-walled jet of 49μ bore with a pressure of 100 cm. produced bubbles of 1.2 mm. in diameter. A thin-walled jet of 27μ diameter and a pressure of 180 cm. produced bubbles of 0.6 mm. diameter. It is convenient to refer to bubbles of 2.0 to 1.0 mm. diameter as 'large' bubbles, those from 0.8 to 0.6 mm. diameter as 'medium' bubbles, and those from 0.3 to 0.1 mm. diameter as 'small' bubbles, since their behaviour varies with their size.

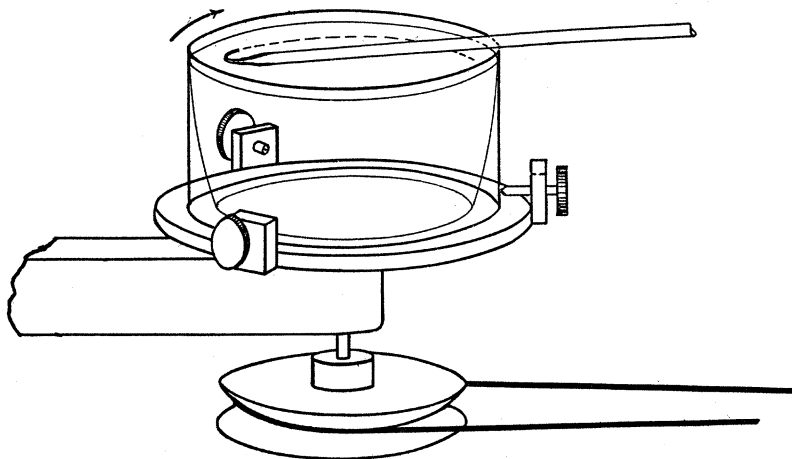


FIGURE 3. Apparatus for producing bubbles of small size.

With this apparatus we have not found it possible to reduce the size of the jet and so produce bubbles of smaller diameter than 0.6 mm. As it was desired to experiment with very small bubbles, we had recourse to placing the soap solution in a rotating vessel and introducing a fine jet as nearly as possible parallel to a stream line. The bubbles are swept away as they form, and under steady conditions are reasonably uniform. They issue at a rate of one thousand or more per second, giving a high-pitched note. The soap solution mounts up in a steep wall around the perimeter of the vessel while it is rotating, but carries back most of the bubbles with it when rotation ceases. With this device, illustrated in figure 3, bubbles down to 0.12 mm. in diameter can be obtained. As an example, an orifice 38μ across in a thin-walled jet, with a pressure of 190 cm. of water, and a speed of the fluid of 180 cm./sec. past the orifice, produced bubbles of 0.14 mm. diameter. In this case a dish of diameter 9.5 cm. and speed of 6 rev./sec. was used. Figure 4, plate 8, is an enlarged picture of these 'small' bubbles and shows their degree of regularity; the pattern is not as perfect with a rotating as with a stationary vessel, the rows being seen to be slightly irregular when viewed in a glancing direction.

These two-dimensional crystals show structures which have been supposed to exist in metals, and simulate effects which have been observed, such as grain boundaries, dislocations and other types of fault, slip, recrystallization, annealing, and strains due to 'foreign' atoms.

3. GRAIN BOUNDARIES

Figures 5*a*, 5*b* and 5*c*, plates 9 and 10, show typical grain boundaries for bubbles of 1.87, 0.76 and 0.30 mm. diameter respectively. The width of the disturbed area at the boundary, where the bubbles have an irregular distribution, is in general greater the smaller the bubbles. In figure 5*a*, which shows portions of several adjacent grains, bubbles at a boundary between two grains adhere definitely to one crystalline arrangement or the other. In figure 5*c* there is a marked 'Beilby layer' between the two grains. The small bubbles, as will be seen, have a greater rigidity than the large ones, and this appears to give rise to more irregularity at the interface.

Separate grains show up distinctly when photographs of polycrystalline rafts such as figures 5*a* to 5*c*, plates 9 and 10, and figures 12*a* to 12*e*, plates 14 to 16, are viewed obliquely. With suitable lighting, the floating raft of bubbles itself when viewed obliquely resembles a polished and etched metal in a remarkable way.

It often happens that some 'impurity atoms', or bubbles which are markedly larger or smaller than the average, are found in a polycrystalline raft, and when this is so a large proportion of them are situated at the grain boundaries. It would be incorrect to say that the irregular bubbles make their way to the boundaries; it is a defect of the model that no diffusion of bubbles through the structure can take place, mutual adjustments of neighbours alone being possible. It appears that the boundaries tend to readjust themselves by the growth of one crystal at the expense of another till they pass through the irregular atoms.

4. DISLOCATIONS

When a single crystal or polycrystalline raft is compressed, extended, or otherwise deformed it exhibits a behaviour very similar to that which has been pictured for metals subjected to strain. Up to a certain limit the model is within its elastic range. Beyond that point it yields by slip along one of the three equally inclined directions of closely packed rows. Slip takes place by the bubbles in one row moving forward over those in the next row by an amount equal to the distance between neighbours. It is very interesting to watch this process taking place. The movement is not simultaneous along the whole row but begins at one end with the appearance of a 'dislocation', where there is locally one more bubble in the rows on one side of the slip line as compared with those on the other. This dislocation then runs along the slip line from one side of the crystal to the other, the final result being a slip by one 'inter-atomic' distance. Such a process has been invoked by Orowan, by Polanyi and by Taylor to explain the small forces required to produce plastic gliding in metal structures. The theory put forward by Taylor (1934) to explain the mechanism of plastic deformation of crystals considers the mutual action and equilibrium of such dislocations. The bubbles afford a very striking picture of what has been supposed to take place in the metal. Sometimes the dislocations run along quite slowly, taking a matter of seconds to cross a crystal; stationary dislocations also are to be seen in crystals which are not homogeneously

strained. They appear as short black lines, and can be seen in the series of photographs, figures 12*a* to 12*e*, plates 14 to 16. When a polycrystalline raft is compressed, these dark lines are seen to be dashing about in all directions across the crystals.

Figures 6*a*, 6*b* and 6*c*, plates 10 and 11, show examples of dislocations. In figure 6*a*, where the diameter of the bubbles is 1.9 mm., the dislocation is very local, extending over about six bubbles. In figure 6*b* (diameter 0.76 mm.) it extends over twelve bubbles, and in figure 6*c* (diameter 0.30 mm.) its influence can be traced for a length of about fifty bubbles. The greater rigidity of the small bubbles leads to longer dislocations. The study of any mass of bubbles shows, however, that there is not a standard length of dislocation for each size. The length depends upon the nature of the strain in the crystal. A boundary between two crystals with corresponding axes at approximately 30° (the maximum angle which can occur) may be regarded as a series of dislocations in alternate rows, and in this case the dislocations are very short. As the angle between the neighbouring crystals decreases, the dislocations occur at wider intervals and at the same time become longer, till one finally has single dislocations in a large body of perfect structure as shown in figures 6*a*, 6*b* and 6*c*.

Figure 7, plate 11, shows three parallel dislocations. If we call them positive and negative (following Taylor) they are positive, negative, positive, reading from left to right. The strip between the last two has three bubbles in excess, as can be seen by looking along the rows in a horizontal direction. Figure 8, plate 12, shows a dislocation projecting from a grain boundary, an effect often observed.

Figure 9, plate 12, shows a place where two bubbles take the place of one. This may be regarded as a limiting case of positive and negative dislocations on neighbouring rows, with the compressive sides of the dislocations facing each other. The contrary case would lead to a hole in the structure, one bubble being missing at the point where the dislocations met.

5. OTHER TYPES OF FAULT

Figure 10, plate 12, shows a narrow strip between two crystals of parallel orientation, the strip being crossed by a number of fault lines where the bubbles are not in close packing. It is in such places as these that recrystallization may be expected. The boundaries approach and the strip is absorbed into a wider area of perfect crystal.

Figures 11*a* to 11*g*, plates 13 and 14 are examples of arrangements which frequently appear in places where there is a local deficiency of bubbles. While a dislocation is seen as a dark stripe in a general view, these structures show up in the shape of the letter V or as triangles. A typical V structure is seen in figure 11*a*. When the model is being distorted, a V structure is formed by two dislocations meeting at an inclination of 60°; it is destroyed by the dislocations continuing along their paths. Figure 11*b* shows a small triangle, which also embodies a dislocation, for it will be noticed that the rows below the fault have one more bubble than those below. If a mild amount

of 'thermal movement' is imposed by gentle agitation of one side of the crystal, such faulty places disappear and a perfect structure is formed.

Here and there in the crystals there is a blank space where a bubble is missing, showing as a black dot in a general view. Examples occur in figure 11*g*. Such a gap cannot be closed by a local readjustment, since filling the hole causes another to appear. Such holes both appear and disappear when the crystal is 'cold-worked'.

These structures in the model suggest that similar local faults may exist in an actual metal. They may play a part in processes such as diffusion or the order-disorder change by reducing energy barriers in their neighbourhood, and act as nuclei for crystallization in an allotropic change.

6. RECRYSTALLIZATION AND ANNEALING

Figures 12*a* to 12*e*, plates 14 to 16, show the same raft of bubbles at successive times. A raft covering the surface of the solution was given a vigorous stirring with a glass rake, and then left to adjust itself. Figure 12*a* shows its aspect about 1 sec. after stirring has ceased. The raft is broken into a number of small 'crystallites'; these are in a high state of non-homogeneous strain as is shown by the numerous dislocations and other faults. The following photograph (figure 12*b*) shows the same raft 32 sec. later. The small grains have coalesced to form larger grains, and much of the strain has disappeared in the process. Recrystallization takes place right through the series, the last three photographs of which show the appearance of the raft 2, 14 and 25 min. after the initial stirring. It is not possible to follow the rearrangement for much longer times, because the bubbles shrink after long standing, apparently due to the diffusion of air through their walls, and they also become thin and tend to burst. No agitation was given to the model during this process. An ever slower process of rearrangement goes on, the movement of the bubbles in one part of the raft setting up strains which activate a rearrangement in a neighbouring part, and that in its turn still another.

A number of interesting points are to be seen in this series. Note the three small grains at the points indicated by the co-ordinates *AA*, *BB*, *CC*. *A* persists, though changed in form, throughout the whole series. *B* is still present after 14 min., but has disappeared in 25 min., leaving behind it four dislocations marking internal strain in the grain. Grain *C* shrinks and finally disappears in figure 12*d*, leaving a hole and a *V* which has disappeared in figure 12*e*. At the same time the ill-defined boundary in figure 12*d* at *DD* has become a definite one in figure 12*e*. Note also the straightening out of the grain boundary in the neighbourhood of *EE* in figures 12*b* to 12*e*. Dislocations of various lengths can be seen, marking all stages between a slight warping of the structure and a definite boundary. Holes where bubbles are missing show up as black dots. Some of these holes are formed or filled up by movements of dislocations, but others represent places where a bubble has burst. Many examples of *V*'s and some of triangles can be seen. Other interesting points will be apparent from a study of this series of photographs.

Figures 13*a*, 13*b* and 13*c*, plate 17, show a portion of a raft 1 sec., 4 sec. and 4 min. after the stirring process, and is interesting as showing two successive stages in the relaxation towards a more perfect arrangement. The changes show up well when one looks in a glancing direction across the page. The arrangement is very broken in figure 13*a*. In figure 13*b* the bubbles have grouped themselves in rows, but the curvature of these rows indicates a high degree of internal strain. In figure 13*c* this strain has been relieved by the formation of a new boundary at *A-A*, the rows on either side now being straight. It would appear that the energy of this strained crystal is greater than that of the intercrystalline boundary. We are indebted to Messrs Kodak for the photographs of figure 13, which were taken when the cinematograph film referred to below was produced.

7. EFFECT OF IMPURITY ATOM

Figure 14, plate 18, shows the widespread effect of a bubble which is of the wrong size. If this figure is compared with the perfect rafts shown in figures 2 and 4, plate 8, it will be seen that three bubbles, one larger and two smaller than normal, disturb the regularity of the rows over the whole of the figure. As has been mentioned above, bubbles of the wrong size are generally found in the grain boundaries, where holes of irregular size occur which can accommodate them.

8. MECHANICAL PROPERTIES OF THE TWO-DIMENSIONAL MODEL

The mechanical properties of a two-dimensional perfect raft have been described in the paper referred to above (Bragg 1942*b*). The raft lies between two parallel springs dipping horizontally in the surface of the soap solution. The pitch of the springs is adjusted to fit the spacing of the rows of bubbles, which then adhere firmly to them. One spring can be translated parallel to itself by a micrometer screw, and the other is supported by two thin vertical glass fibres. The shearing stress can be measured by noting the deflexion of the glass fibres. When subjected to a shearing strain, the raft obeys Hooke's law of elasticity up to the point where the elastic limit is reached. It then slips along some intermediate row by an amount equal to the width of one bubble. The elastic shear and slip can be repeated several times. The elastic limit is approximately reached when one side of the raft has been sheared by an amount equal to a bubble width past the other side. This feature supports the basic assumption made by one of us in the calculation of the elastic limit of a metal (Bragg 1942*a*), in which it is supposed that each crystallite in a cold-worked metal only yields when the strain in it has reached such a value that energy is released by the slip.

A calculation has been made by M. M. Nicolson of the forces between the bubbles, and will be published shortly. It shows two interesting points. The curve for the variation of potential energy with distance between centres is very similar to those which have been plotted for atoms. It has a minimum for a distance between centres slightly less than a free bubble diameter, and rises sharply for smaller distances. Further, the rise is extremely sharp for bubbles of 0.1 mm. diameter but

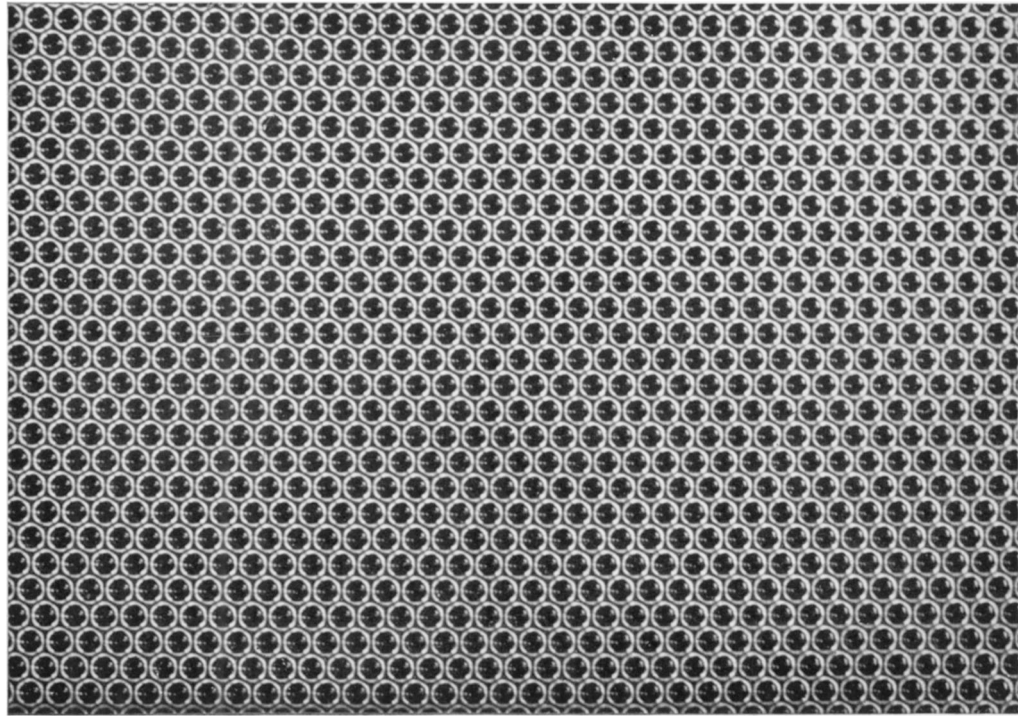


FIGURE 2. Perfect crystalline raft of bubbles. Diameter 1.41 mm.

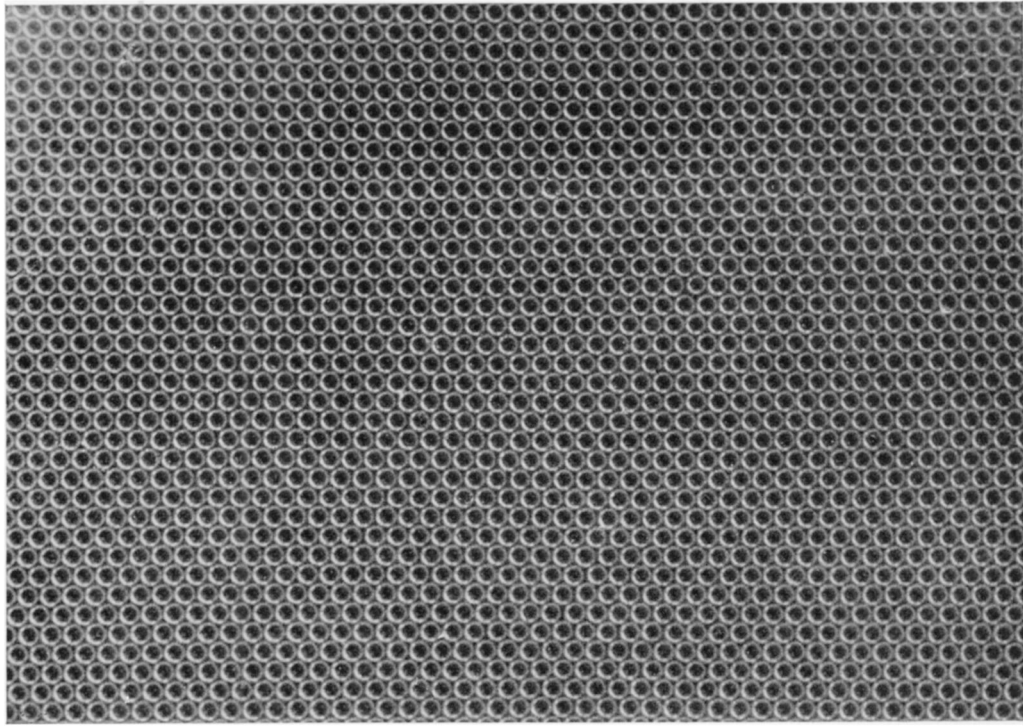


FIGURE 4. Perfect crystalline raft of bubbles. Diameter 0.30 mm.

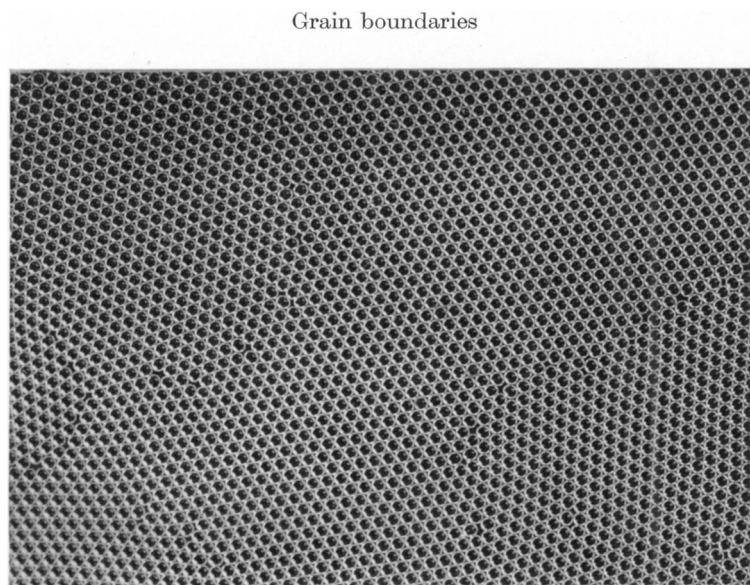


FIGURE 5*a*. Diameter 1.87 mm.

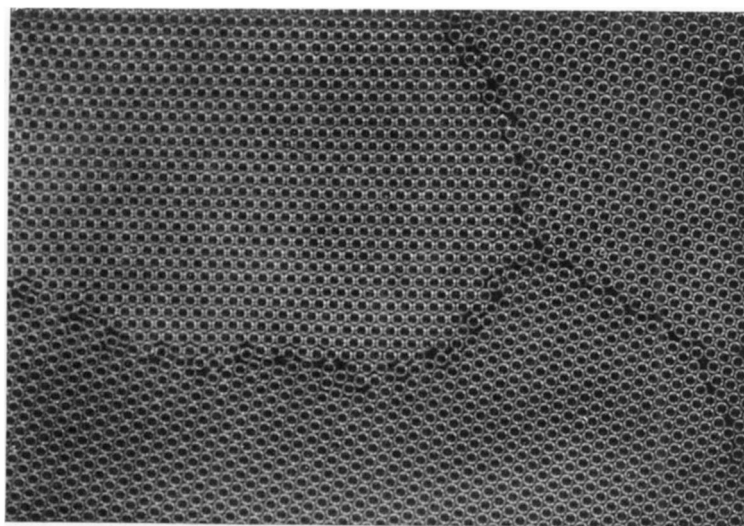


FIGURE 5*b*. Diameter 0.76 mm.

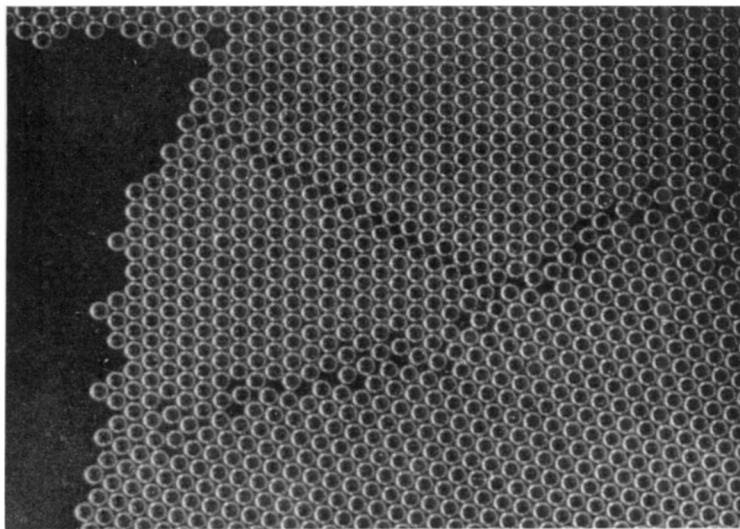


FIGURE 5*c*. A grain boundary. Diameter 0.30 mm.

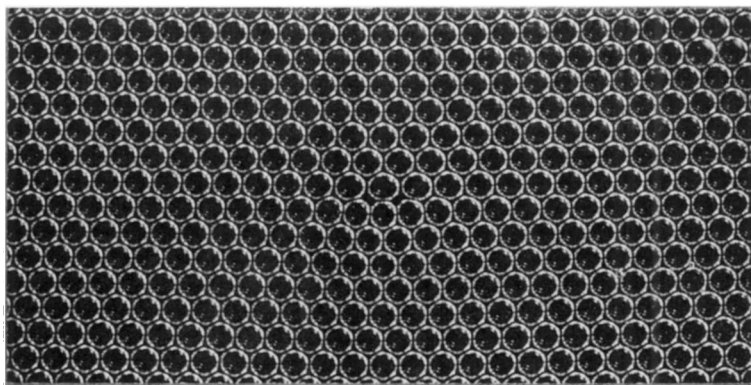


FIGURE 6*a*. A dislocation. Diameter 1.9 mm.

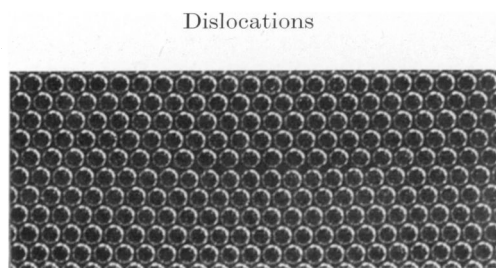


FIGURE 6*b*. Diameter 0.76 mm.

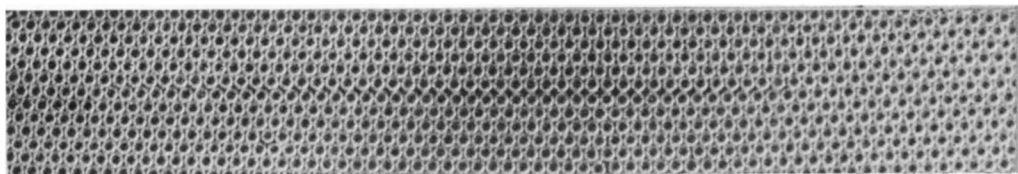


FIGURE 6*c*. Diameter 0.30 mm.

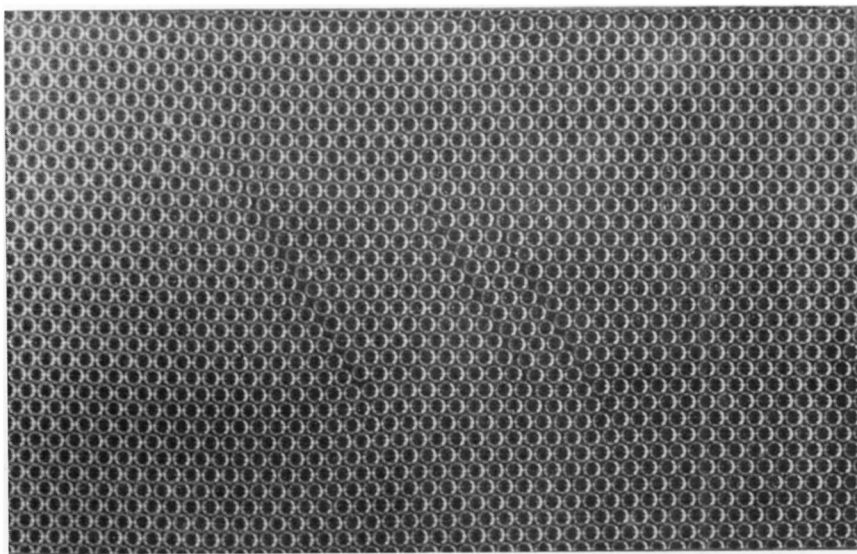


FIGURE 7. Parallel dislocations. Diameter 0.76 mm.

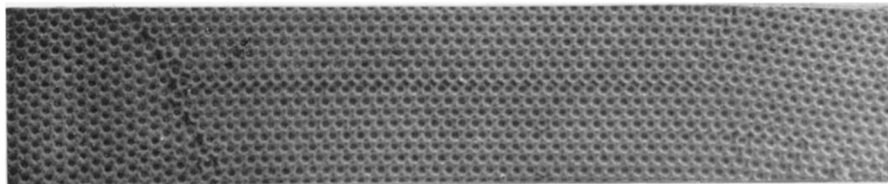


FIGURE 8. Dislocation projecting from a grain boundary. Diameter 0.30 mm.

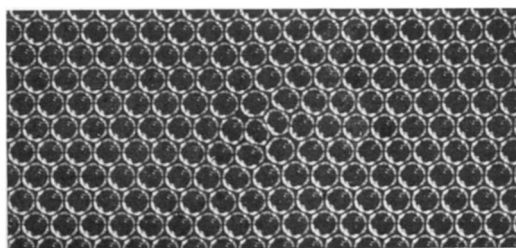


FIGURE 9. Dislocations in adjacent rows. Diameter 1.9 mm.

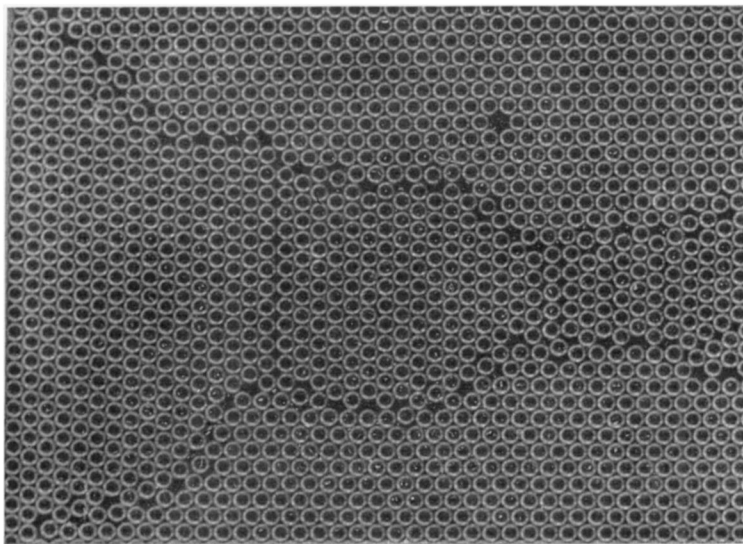
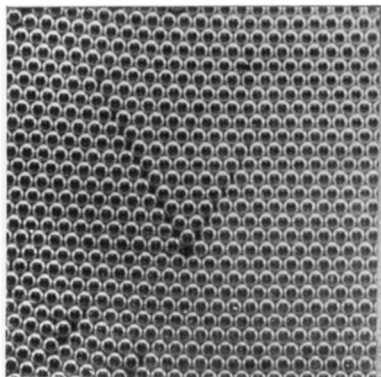
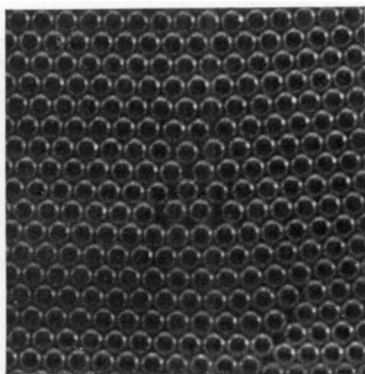


FIGURE 10. Series of fault lines between two areas of parallel orientation. Diameter 0.30 mm.



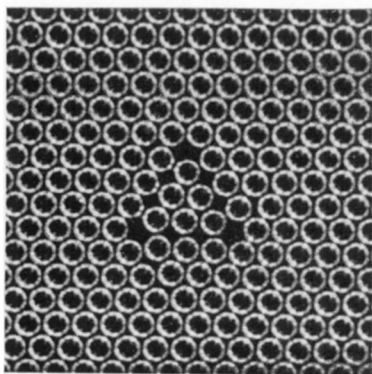
Diameter 0.68 mm.

a



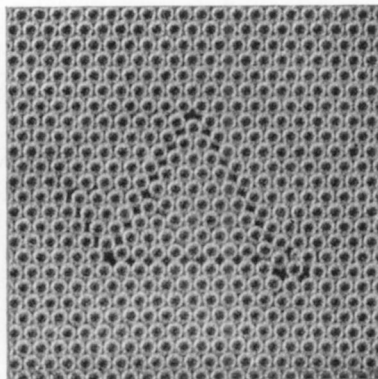
Diameter 0.68 mm.

b



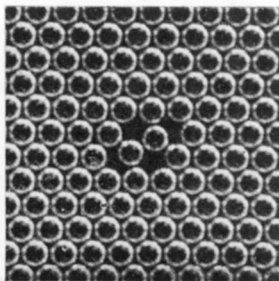
Diameter 0.6 mm.

c



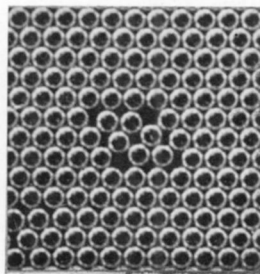
Diameter 0.30 mm.

d



Diameter 0.6 mm.

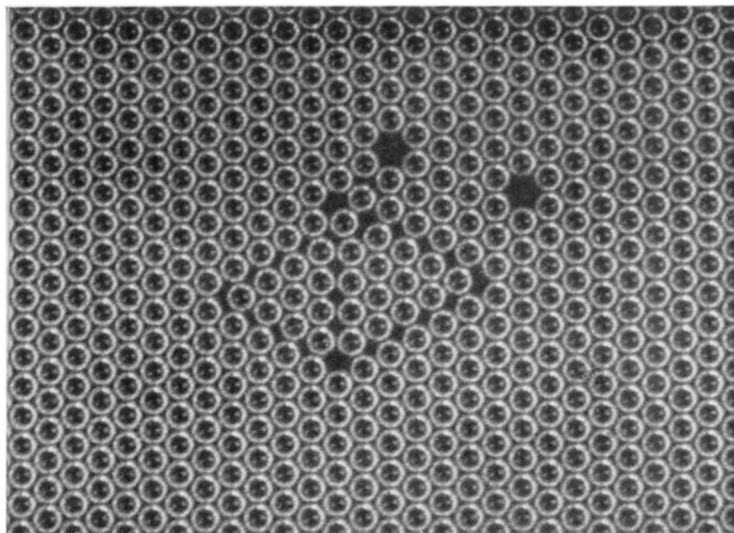
e



Diameter 0.6 mm.

f

FIGURE 11. Types of fault.



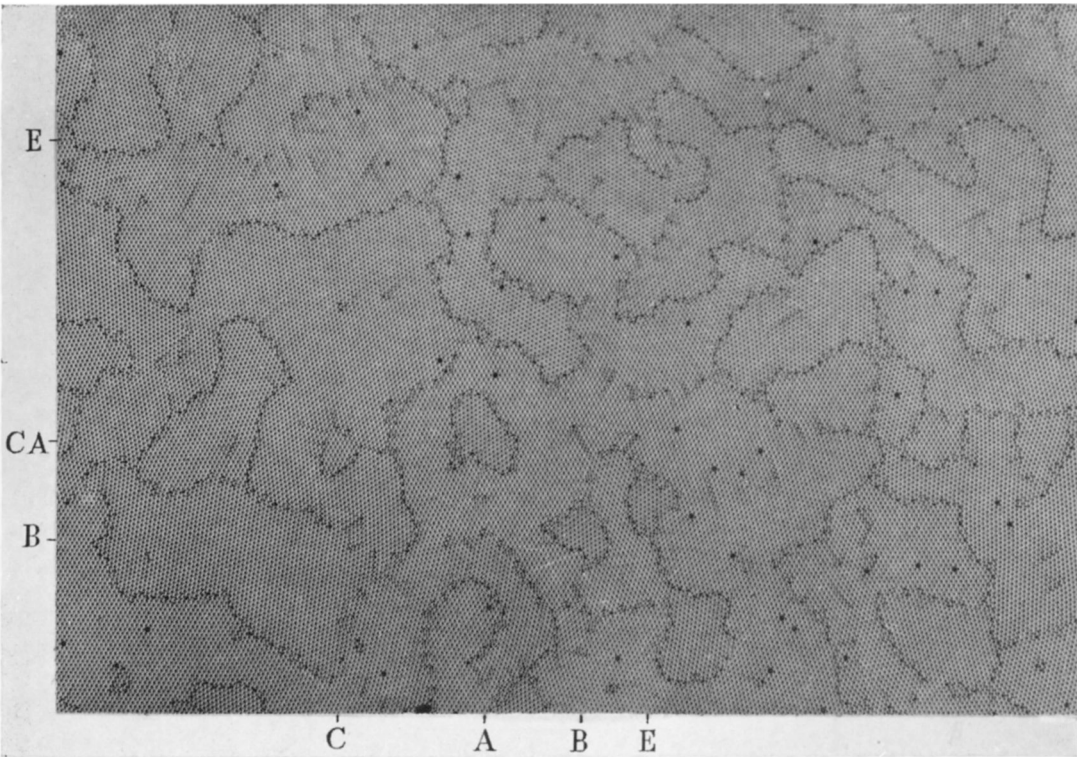
g

FIGURE 11. Types of fault. Diameter 0.68 mm.

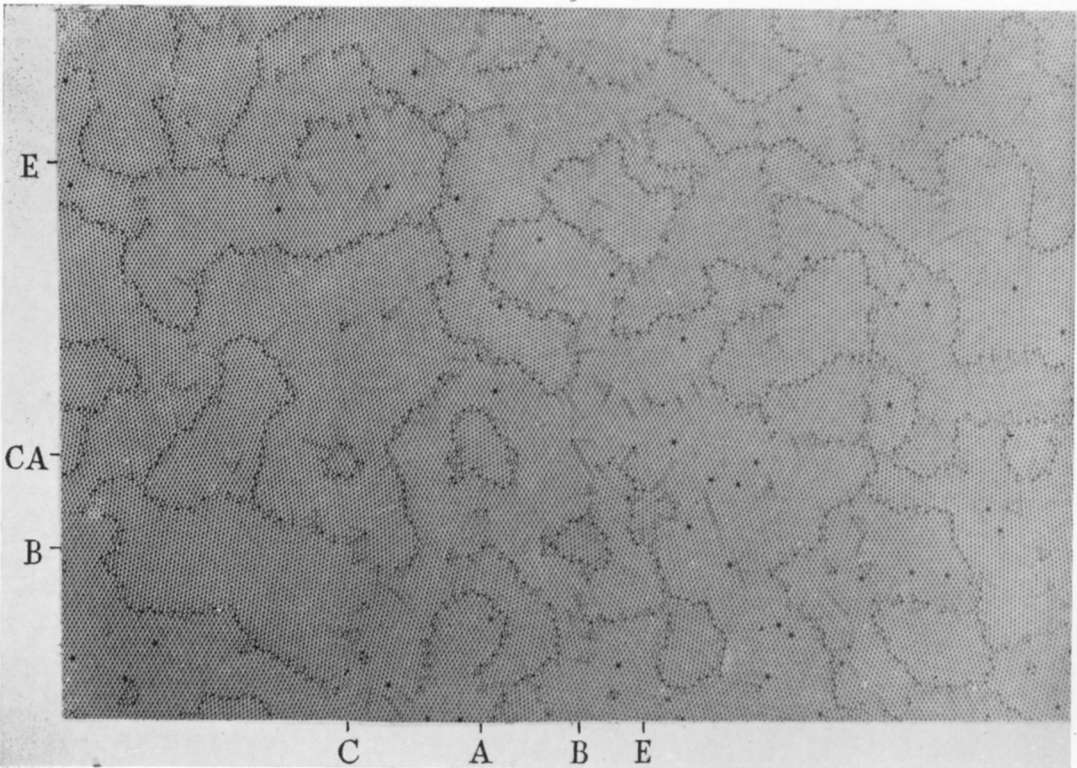


a. Immediately after stirring.

FIGURE 12. Recrystallization. Diameter 0.60 mm.

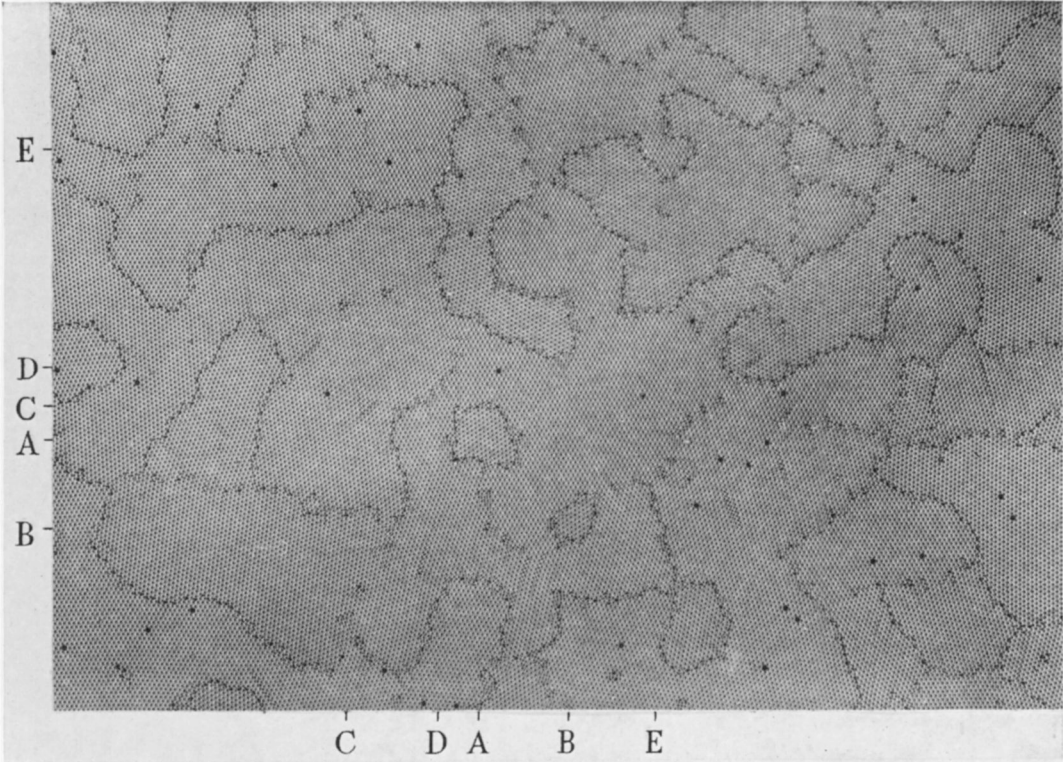


b. After 33 sec.

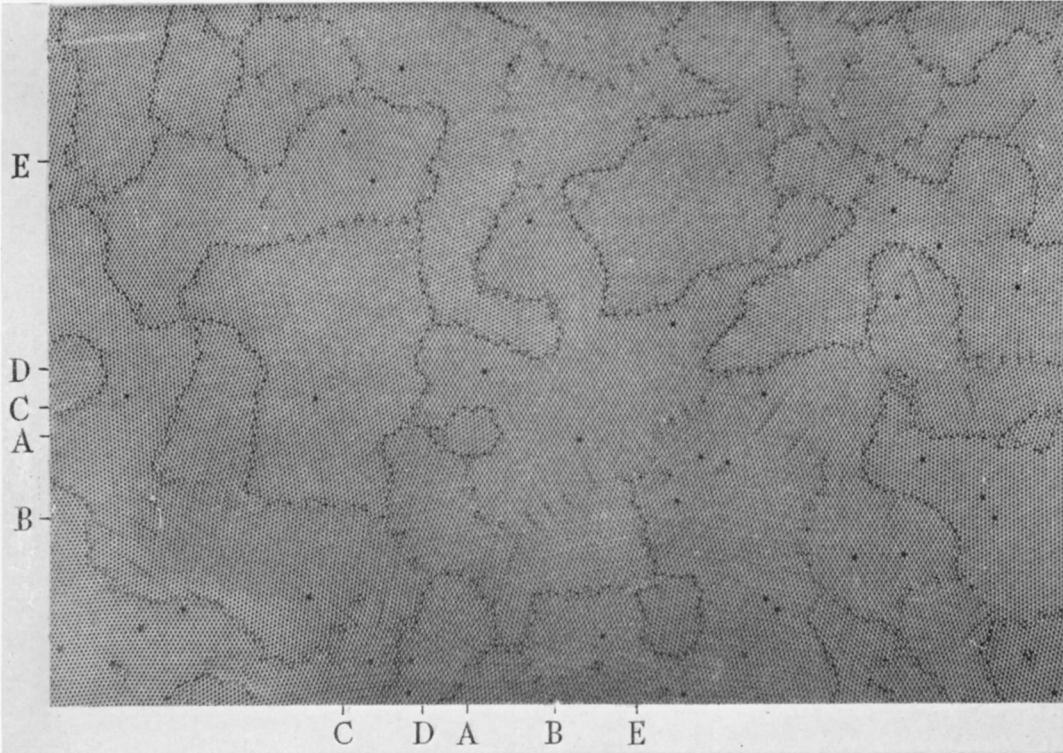


c. After 2 min.

FIGURE 12

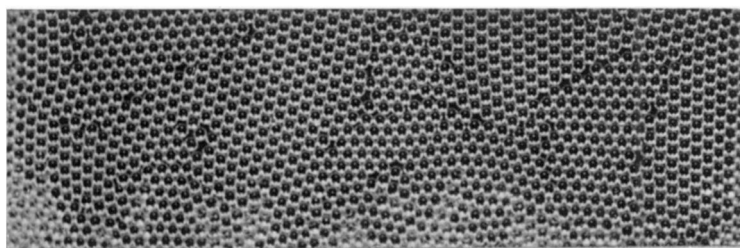


d. After 14 min.

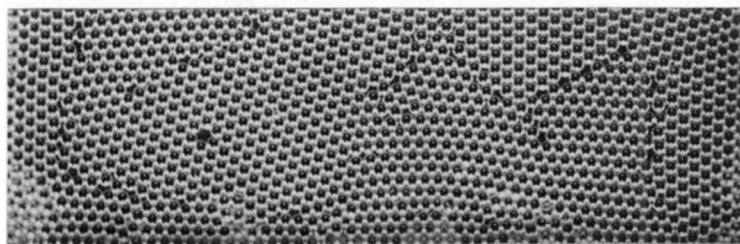


e. After 25 min.

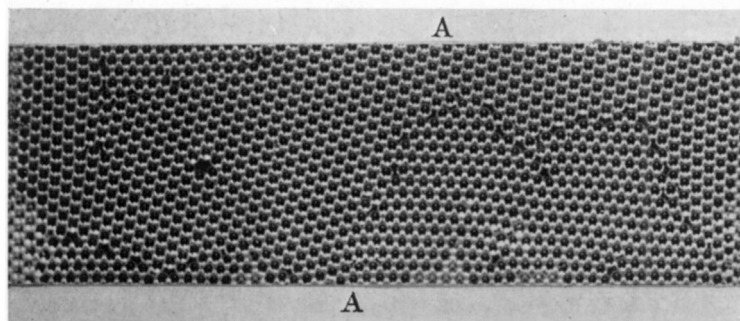
FIGURE 12



a After 1 sec.



b After 4 sec.



c After 4 min.

FIGURE 13. Two stages of recrystallization. Diameter 1.64 mm.

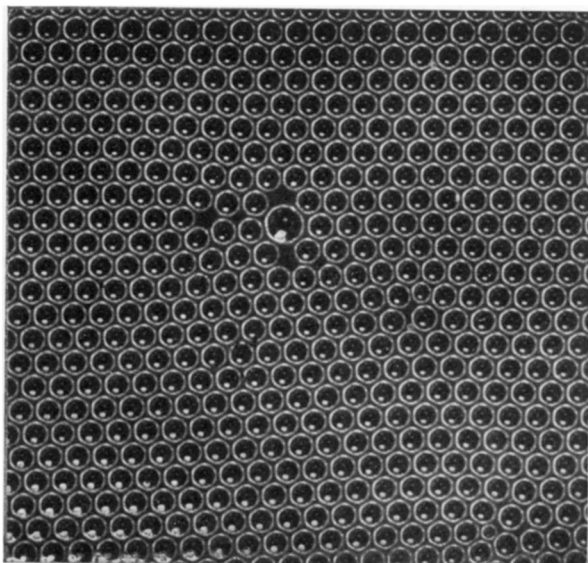


FIGURE 14. Effect of atoms of impurity. Diameter of uniform bubbles about 1.3 mm.

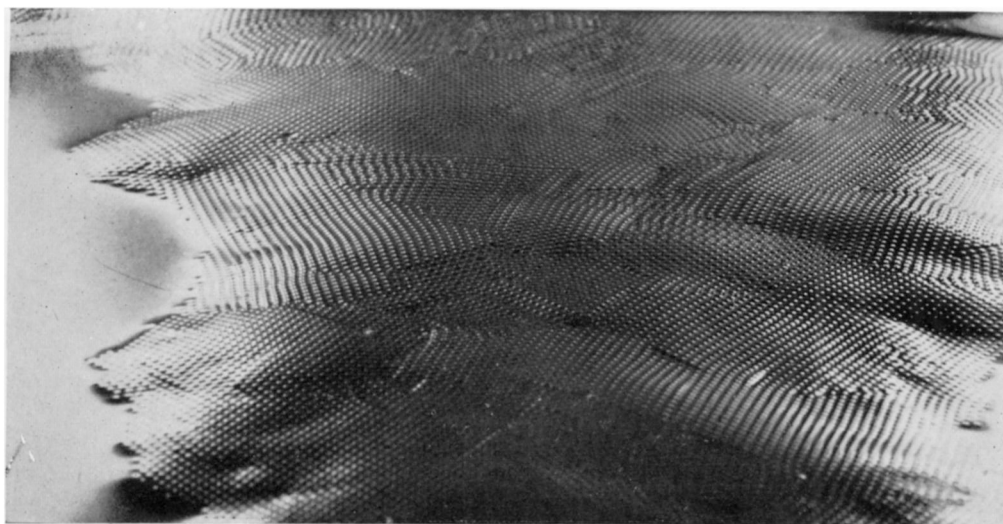
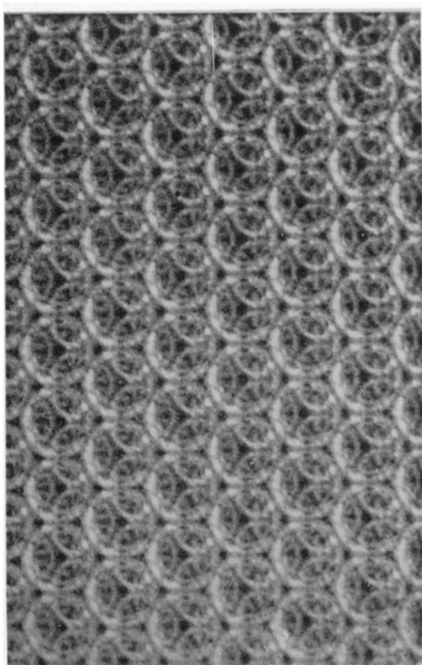
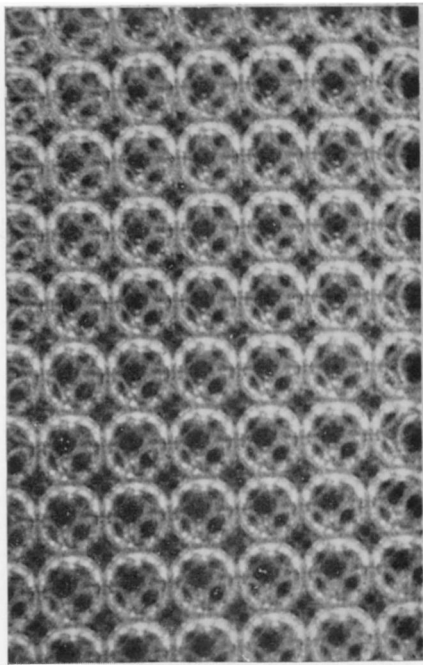


FIGURE 15. Oblique view of three-dimensional raft.

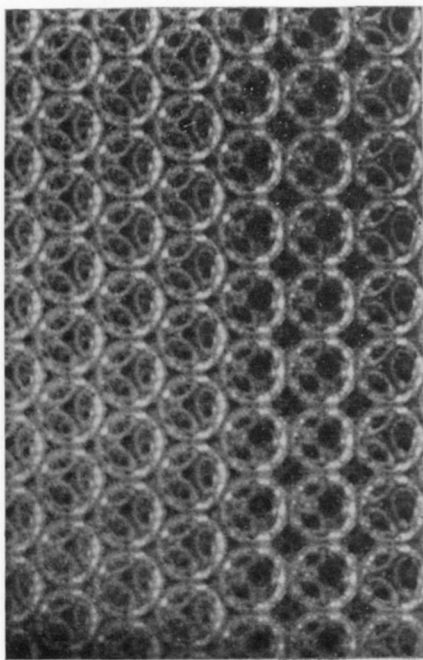


a. (111) face.

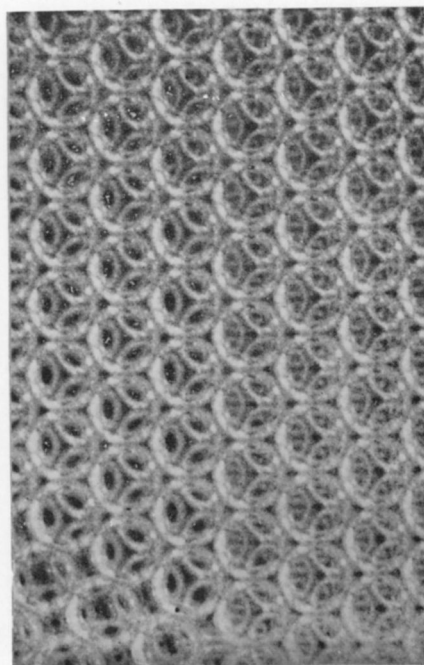


b. (100) face.

Face-centred cubic structure.



c. Twin across (111), cubic structure.



d. Possible example of hexagonal close-packing.

Diameter 0.70 mm.

FIGURE 17

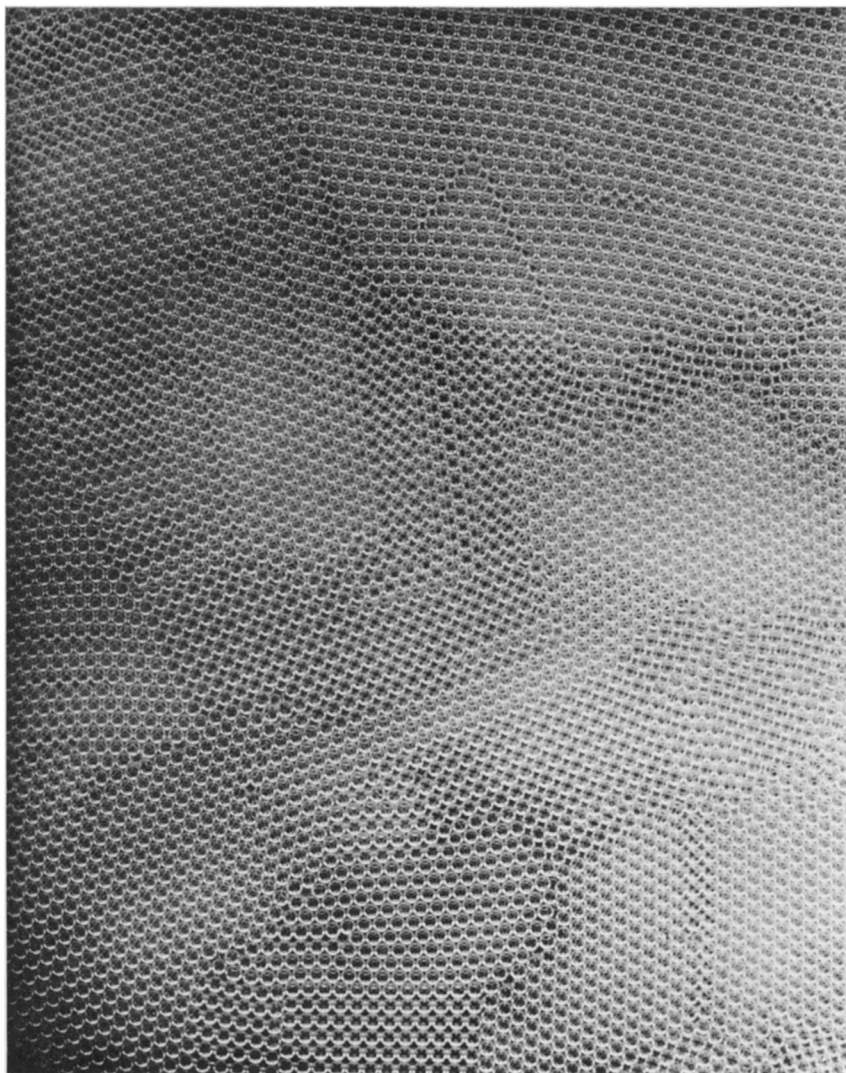


FIGURE 16. A three-dimensional raft viewed normally. Diameter 0.70 mm.

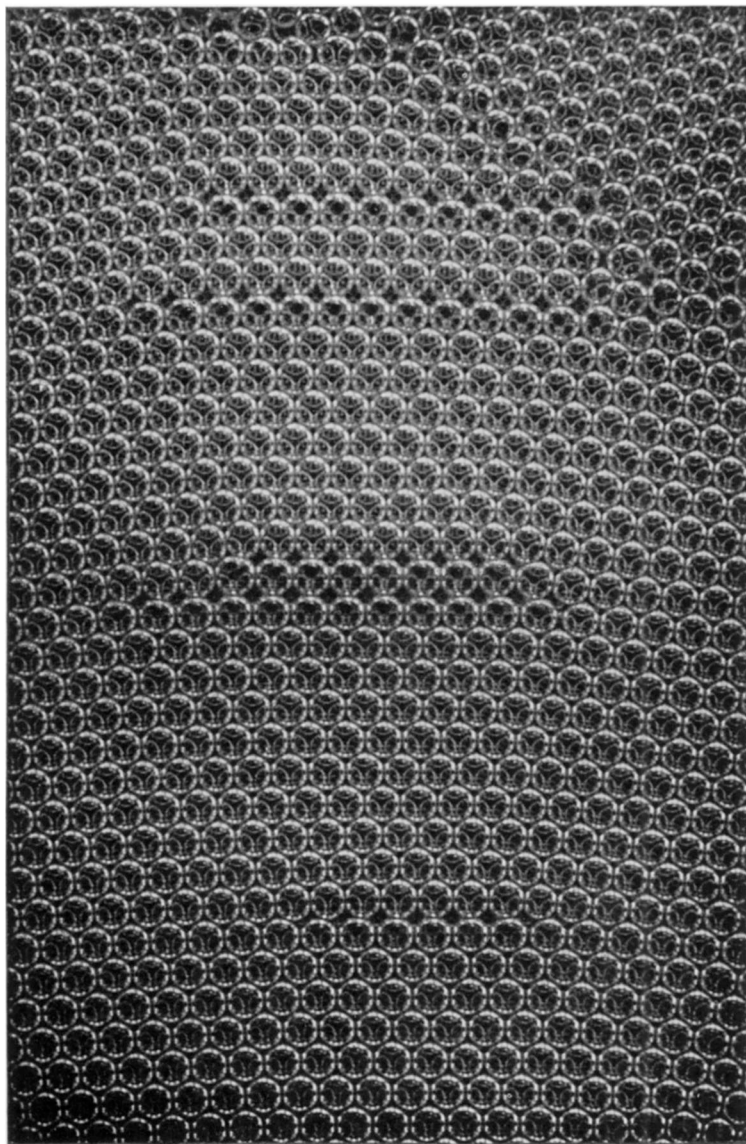


FIGURE 18. Dislocations in three-dimensional structure. Diameter 0.70 mm.

much less so for bubbles of 1 mm. diameter, thus confirming the impression given by the model that the small bubbles behave as if they were much more rigid than the large ones.

9. THREE-DIMENSIONAL ASSEMBLAGES

If the bubbles are allowed to accumulate in multiple layers on the surface, they form a mass of three-dimensional 'crystals' with one of the arrangements of closest packing. Figure 15, plate 18, shows an oblique view of such a mass; its resemblance to a polished and etched metal surface is noticeable. In figure 16, plate 20, a similar mass is seen viewed normally. Parts of the structure are definitely in cubic closest packing, the outer surface being the (111) face or (100) face. Figure 17*a*, plate 19, shows a (111) face. The outlines of the three bubbles on which each upper bubble rests can be clearly seen, and the next layer of these bubbles is faintly visible in a position not beneath the uppermost layer, showing that the packing of the (111) planes has the well-known cubic succession. Figure 17*b*, plate 19, shows a (100) face with each bubble resting on four others. The cubic axes are of course inclined at 45° to the close-packed rows of the surface layer. Figure 17*c*, plate 19, shows a twin in the cubic structure across the face (111). The uppermost faces are (111) and (100), and they make a small angle with each other, though this is not apparent in the figure; it shows up in an oblique view. Figure 17*d*, plate 19, appears to show both the cubic and hexagonal succession of closely packed planes, but it is difficult to verify whether the left-hand side follows the true hexagonal close-packed structure because it is not certain that the assemblage had a depth of more than two layers at this point. Many instances of twins, and of intercrystalline boundaries, can be seen in figure 16, plate 20.

Figure 18, plate 21, shows several dislocations in a three-dimensional structure subjected to a bending strain.

10. DEMONSTRATION OF THE MODEL

With the co-operation of Messrs Kodak, a 16 mm. cinematograph film has been made of the movements of the dislocations and grain boundaries when single crystal and polycrystalline rafts are sheared, compressed, or extended. Moreover, if the soap solution is placed in a glass vessel with a flat bottom, the model lends itself to projection on a large scale by transmitted light. Since a certain depth is required for producing the bubbles, and the solution is rather opaque, it is desirable to make the projection through a glass block resting on the bottom of the vessel and just submerged beneath the surface.

In conclusion, we wish to express our thanks to Mr C. E. Harrold, of King's College, Cambridge, who made for us some of the pipettes which were used to produce the bubbles.

REFERENCES

- Bragg, W. L. 1942*a* *Nature*, **149**, 511.
Bragg, W. L. 1942*b* *J. Sci. Instrum.* **19**, 148.
Taylor, G. I. 1934 *Proc. Roy. Soc. A*, **145**, 362.

LINKED CITATIONS

- Page 1 of 1 -



You have printed the following article:

A Dynamical Model of a Crystal Structure

Lawrence Bragg; J. F. Nye

Proceedings of the Royal Society of London. Series A, Mathematical and Physical Sciences, Vol. 190, No. 1023. (Sep. 9, 1947), pp. 474-481.

Stable URL:

<http://links.jstor.org/sici?sici=0080-4630%2819470909%29190%3A1023%3C474%3AADMOAC%3E2.0.CO%3B2-D>

This article references the following linked citations. If you are trying to access articles from an off-campus location, you may be required to first logon via your library web site to access JSTOR. Please visit your library's website or contact a librarian to learn about options for remote access to JSTOR.

References

The Mechanism of Plastic Deformation of Crystals. Part I. Theoretical

G. I. Taylor

Proceedings of the Royal Society of London. Series A, Containing Papers of a Mathematical and Physical Character, Vol. 145, No. 855. (Jul. 2, 1934), pp. 362-387.

Stable URL:

<http://links.jstor.org/sici?sici=0950-1207%2819340702%29145%3A855%3C362%3ATMOPDO%3E2.0.CO%3B2-4>